THE JOURNAL OF PHYSICAL CHEMISTRY A

Subscriber access provided by UZH Hauptbibliothek / Zentralbibliothek Zuerich

Article

Electronic Properties of FC(O)SCH2CH3. A Combined He(I) Photoelectron Spectroscopy and Synchrotron Radiation Study

Lucas Sebastián Rodríguez Pirani, Mauricio Federico Erben, Mariana Geronés, Rosana Mariel Romano, Reinaldo Luiz Cavasso Filho, Chunping Ma, Maofa Ge, and Carlos Omar Della Védova

J. Phys. Chem. A, **Just Accepted Manuscript** • DOI: 10.1021/jp412564u • Publication Date (Web): 14 Jul 2014

Electronic Properties of $FC(O)SCH_2CH_3$. A Combined He(I) Photoelectron Spectroscopy and Synchrotron Radiation Study

Lucas S. Rodríguez Pirani,[‡] Mauricio F. Erben,[‡,] Mariana Geronés,[‡] Rosana M. Romano,[‡] Reinaldo L. Cavasso Filho,[£] Chunping Ma,[&] Maofa Ge,[&] and Carlos O. Della Védova [‡,]**

[‡]CEQUINOR (CONICET-UNLP). Departamento de Química. Facultad de Ciencias Exactas. Universidad Nacional de La Plata, C. C. 962 (1900) La Plata, República Argentina.

[£] Universidade Federal do ABC, Rua Catequese, 242, CEP: 09090-400, Santo André, São Paulo, Brazil.

[&] State Key Laboratory for Structural Chemistry of Unstable and Stable Species, Beijing National Laboratory for Molecular Sciences (BNLMS), Institute of Chemistry, Chinese Academy of Sciences, Beijing 100190, Peoples Republic of China.

Kewwords: S-alquil halo(thioformates), photoionization, PEPICO, PEPIPICO, computational chemistry

*To whom correspondence should be addressed. E-mail: (CODV) carlosdv@quimica.unlp.edu.ar, (MFE) erben@quimica.unlp.edu.ar.

1-Abstract

The valence electronic properties of S-ethyl fluorothioformate (S-ethyl fluoromethanethioate), $FC(O)SCH_2CH_3$, were investigated by means of He(I) photoelectron spectroscopy in conjunction with the analysis of the photofragmentation products determined by PEPICO (Photoelectron Photoion Coincidence) by using synchrotron radiation in the 11.1-21.6 eV photon energy range. The first band observed at 10.28 eV in the HeI photoelectron spectrum can be assigned with confidence to the ionization process from the HOMO [n_π(S) orbital], which is described as a lone pair formally localized on the sulfur atom, in agreement with quantum chemical calculations using the Outer Valence Green's Function method [OVGF/6-311++G (d,p)]. One of the most important fragmentation channels also observed in the valence region corresponds the decarbonylation process yielding the $[M–CO]^{\cdot+}$ ion, which is clearly observed at m/z= 80. Moreover, S 2p and S 2s absorption edges have been examined by measuring the Total Ion Yield spectra in the 160-240 eV region using variable synchrotron radiation. The dynamic of ionic fragmentation following the Auger electronic decay has been evaluated with the help of the PEPIPICO (Photoion-Photoion-Photoelectron-Coincidence spectra) technique.

2-Introduction

Very detailed studies on the photoionization and dissociative ionization processes of molecules in the gas phase can be accomplished by using synchrotron radiation and mass-spectrometry techniques in the multicoincidence mode.[1] These include fundamental and applied aspects, such as the determination of accurate thermodynamic parameters,[2] radiation induce damage of biological molecules,[3,4] combustion chemistry[5] and simple radicals[6] and model compounds,[7,8] among others.

In particular, the ionic dissociation of S-alkyl thioformates, HC(O)SR (R= alkyl), upon electron impact conditions were early studied by Flammang, Nguyen and co-workers by using sophisticated mass-spectrometry based methodologies.[9-11] Interestingly, the $^{\bullet}CH_2CH_2SH_2^+$ β-distonic radical cation was detected as the product of decarbonylation of $HC(O)SCH_2CH_3$ in the 70 eV electron-impact mass-spectrum.[10] The interest in this species begins because the close related oxygenated analogue, i.e. the β-distonic radical cation of ethanol, $^{\bullet}CH_2CH_2OH_2^+$, was computed to be about 42 kJ/mol more stable than the classical radical cation.[9,10,12] More recently, the ionization process of thioethanol toward the formation of both the conventional radical cation ($CH_3CH_2SH^{\cdot+}$) and the distonic isomer, $^{\bullet}CH_2CH_2SH_2^+$, were investigated by means of high level ab initio methods, showing that the distonic radical cation is slightly less stable than the conventional ones.[13]

These remarkable features found for sulfur containing species prompted us to study the dissociation dynamic of S-alkyl halothioformate [XC(O)SR, X= halogen, R= $-CH_3$, $-CH_2CH_3$].[14-17] Thus, in a previous work we reported the photoionization behavior of $ClC(O)SCH_2CH_3$ upon VUV and soft-X ray photon impact.[14] Following the previous reports on the close related $HC(O)SCH_2CH_3$ molecule,[9-11] special attention was paid to the recognition of ionic fragments arising from decarbonylation process (see

Scheme 1). However, the $(M–28)^+$ fragment is not observed in our spectra neither in the valence nor inner-shell regions. Therefore, the decarbonylation is precluded when hydrogen in $HC(O)SCH_2CH_3$ is changed by a chlorine atom in $ClC(O)SCH_2CH_3$. We concluded that it is likely that migration of heavy atoms -like chlorine- disfavored the first step proposed for the decarbonylation, i.e. formation of the intermediate sulfurane ion.[10]

Scheme 1. Decarbonylation process from $XC(O)SCH_2CH_3$ molecule (X=H, F)

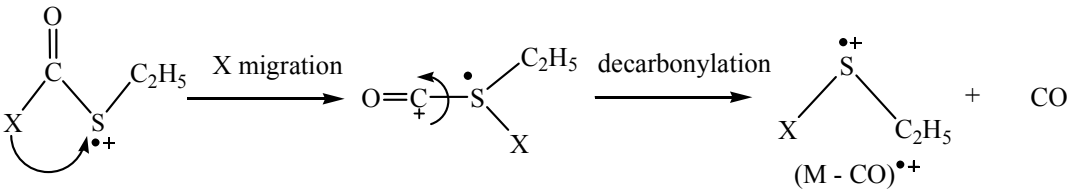

In the present work, photoionization studies have been conducted for the related molecule $FC(O)SCH_2CH_3$. The choice of the title species is mainly given by the low mass of the fluorine atom and a wide range of photon energies is applied, which includes the He(I) photoelectron spectra as well as synchrotron-based studies on the valence and the inner-shell S 2p edge.

3-Experimental Section

A toroidal grating monochromator available at the TGM beam line (Laboratório Nacional de Luz Síncrotron, LNLS, Campinas, Brazil)[18] was used. This provide linearly polarized light in the range 12-310 eV[19] intersecting the effusive gaseous sample in a perpendicular arrangement. The base pressure at the high-vacuum chamber was in the range of 10^{-8} mbar and during the experiments, the pressure was maintained below 2×10^{-6} mbar. The photon energy resolution from 12 to 21.5 eV was given by $E/\Delta E = 550$ and better than 400 for the S 2p region. Gaseous SF_6 was used for energy calibration.[20]

The intensity of the emergent beam was recorded by a light-sensitive diode. The Time-Of-Flight (TOF) mass spectrometer for both PEPICO and PEPIPICO measurements[21,22] was discussed elsewhere.[23] A Multi Channel Plate (MCP) perceives the accelerated electrons which are recorded without energy analysis. A gas-phase harmonic filter was used in the 12-21.5 eV region in order to avoid contamination of the photon beam with high-order harmonics.[24-26]

The average kinetic energy release (KER) values of the fragments were evaluated from the coincidence spectra by assuming ideal conditions, including isotropic distribution of the fragments, that they are perfectly space-focused and that the electric field applied in the extraction region is uniform.[27] Under these conditions, the KER in the fragmentation process can be determined from the peak width following the method suggested by Pilling et. al[28] and eventual deviations from these conditions tend to increase the peak width, and thus the values calculated can be considered as upper bounds. Santos et. al[29] have measured the argon TOF spectrum using the same experimental setup, and a peak width value of 0.05 eV was achieved for the Ar^+ ion. This value represents a good estimation for the instrumental resolution since the broadening in argon can only be the result of thermal energy and instrument broadening.

A double-chamber UPS-II machine at a resolution of about 30 meV was used to record the HeI PE spectrum of $FC(O)SCH_2CH_3$. The UPS apparatus used here utilizes the usual detection geometry, in which the detector located at right angle respect to the incident light beam from the He(I) lamp. The resolution was measured using the $Ar^+(^2P_{3/2})$ photoelectron band.[30-35] Experimental vertical ionization energies (I_v in eV) were calibrated using a small amounts of argon or iodomethane to the sample.

$FC(O)SCH_2CH_3$ has been computed in its ground electronic state using the Gaussian03 program package using OVGF calculations[36] and the 6-311++G(d,p) basis set and B3LYP/6-311++G(d,p)-optimized geometry of the most stable rotamer.[37]

The UB3LYP/6-311++G(d,p) level of approximation was used in order to compute the dissociation energies of the $FC(O)SCH_2CH_3^{\bullet+}$ parent radical ion into possible fragments.

S-ethyl fluorothioformate, $FC(O)SCH_2CH_3$, can be obtained by reacting S-ethyl chlorothioformate, $ClC(O)SCH_2CH_3$, with thallium fluorine, according to the following reaction:

$$ClC(O)SCH_2CH_3 + TlF \rightarrow FC(O)SCH_2CH_3 + TlCl$$

Consolidated vacuum techniques were employed to condense S-ethyl chlorothioformate over TlF into a 90 mL glass tube. Then, the mixture of reaction was heated up to 70 °C for seven hours and the reaction products were separated by vacuum fractionation through traps at -30, -60, and -196 °C. $FC(O)SCH_2CH_3$ is retained as a pale-yellow liquid in the -60 ºC trap. The yield of reaction was nearly quantitative. S-ethyl chlorothioformate was synthesized using triphosgene and ethanethiol in presence of triethylamine.[38] The liquid products were purified by distillation followed by trap-to-trap condensation at reduced pressure and carefully checked by IR (vapor) and Raman (liquid)[39] spectroscopy. In particular, the title molecule has been exhaustively characterized by several techniques, such as FTIR, Raman, ^1H and ^{19}F NMR spectroscopies (See Supporting Information).

4-Results and Discussion

4.1-Valence electron region

It is well-known that the molecular conformation affects the ionization energies in the valence region.[40-42] The first investigations related with the conformational properties of ethyl thioesters of general formula $XC(O)SCH_2CH_3$ (X= H, Cl, F, CN, CF_3) had been performed by True and Bohn by using low resolution microwave spectroscopy.[43] In all cases, the *synperiplanar* structure around XC(O)SC- skeleton –with the C=O double bond and the S–C single bond mutually oriented in syn orientation–, is more stable than *antiperiplanar* structure. Moreover, ethyl derivatives can adopt also different conformations depending on the orientation of the $-CH_2CH_3$ group, represented by different C-S-C-C dihedral angle values. For $FC(O)SCH_2CH_3$, the low resolution microwave spectrum was analyzed on the basis of the presence of two rotamers displaying *syn* conformation of the O=C-S-C dihedral angle and *gauche* or *anti* conformations of the ethyl chain.[43] We performed quantum chemical calculations at the B3LYP/aug-cc-pVTZ level of approximation and obtained a qualitative agreement with this conformational landscape. Thus, the most stable conformation of $FC(O)SCH_2CH_3$ in the ground electronic state is the *syn-gauche* conformer (C_1 symmetry point group), while the *syn-anti* form (C_S symmetry point group) is computed 0.33 kcal/mol higher in energy (ΔE^0 value). A third conformer, corresponding to an *anti-gauche* orientation, is calculated at 2.2 kcal/mol above the most stable form (ΔE^0 value). Taken into account the double-degeneracy of the gauche form, the expected conformational ratio between these conformers at room temperature is 63:35:2. This conformational ratio was obtained from the Boltzmann distribution taking into consideration the free energy differences value, ΔG^0, computed at the B3LYP/aug-cc-pVTZ level of approximation (See Supporting Information). Accordingly, at least the

syn-gauche and *syn-anti* conformers are expected to be present in the experiments in significant concentration. For the latter, all canonical molecular orbitals of type a' are σ-orbitals lying in the molecular plane, while those of type a" are π-orbitals. On the basis of the independent particle description, the 36 valence electrons can be paired in 18 doubly occupied orbital. The photoelectron spectrum of $FC(O)SCH_2CH_3$ is conveniently discussed in terms of vertical transitions with reference to these ground-state configurations.

4.1.1-Photoelectron Spectra. The PE spectrum of $FC(O)SCH_2CH_3$ is shown in the Figure 1, while the experimental and theoretical ionization energies and pole strengths are listed in Table 1. The results obtained from the OVGF/6-311++G(d,p) calculations (syn-gauche and syn-anti conformers optimized at the B3LYP/6-311++G(d,p) level of approximation) were used for the assignments of PE spectrum bands to photoionization processes from specific molecular orbitals. Very similar ionization values are computed for both conformers, making difficult to assign the observed ionization bands to individual conformations. A similar limitation was reported early by Turchaninov for related compounds.[44] Thus, the characters of the highest occupied molecular orbital for the energetically most stable syn-gauche conformer of $FC(O)SCH_2CH_3$ are shown in Figure 2.

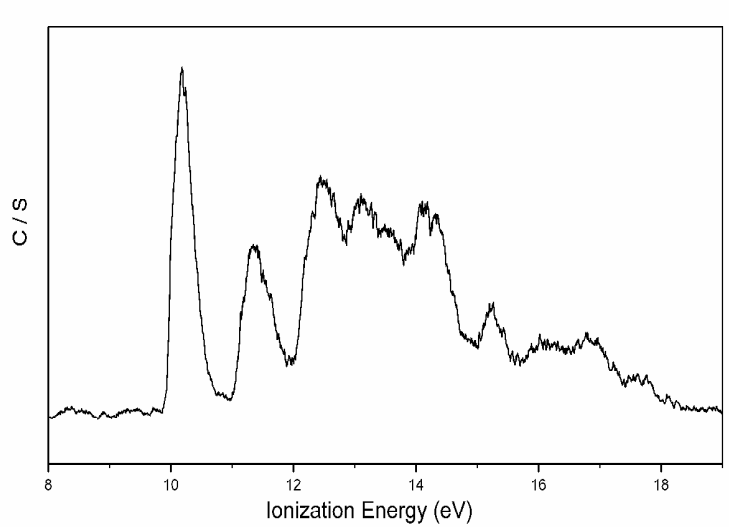

Figure 1. HeI photoelectron spectrum of $FC(O)SCH_2CH_3$.

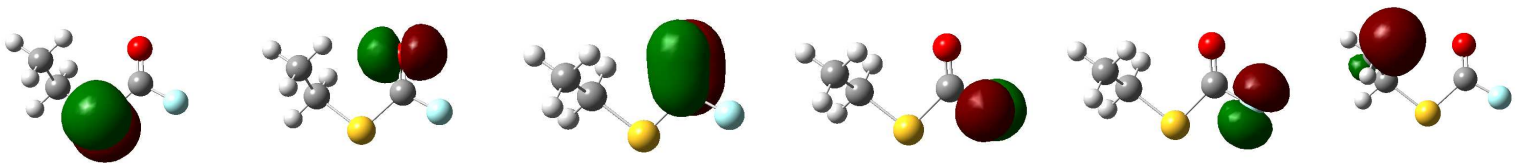

HOMO, n_π(S)	HOMO-1, n_σ(O)	HOMO-2, π (C=O)	HOMO-3, n_π (F)	HOMO-4, n_σ (F)	HOMO-5, $\sigma_{C\text{-}H}$(-CH_3)
MO 28	MO 27	MO 26	MO 25	MO 24	MO 23

Figure 2. Character of the six highest occupied orbitals of $FC(O)SCH_2CH_3$.

Table 1. Experimental and Computed Ionization Energies (eV) and MO Characters for $FC(O)SCH_2CH_3$.

PES (eV)	Calculated (eV)		MO	Character
	OVGF/6-311++G (d,p)			
	syn-gauche	syn-anti		
10.18	10.01 (0.91)	9.99 (0.91)	28	$n_\pi(S)$
11.37	11.55 (0.90)	11.57 (0.90)	27	$n_\sigma(O)$
12.46	12.48 (0.90)	12.49 (0.89)	26	$\pi(C=O)$
13.11	13.19 (0.91)	13.44 (0.91)	25	$n_\pi(F)$
13.56	13.85 (0.89)	13.64 (0.89)	24	$n_\sigma(F)$
14.10	14.15 (0.88)	14.07 (0.87)	23	$\sigma_{C-H}(-CH_3)$

[a] Values calculated at OVGF/6-311++G(d,p) level of approximation with B3LYP/6-311++G(d,p) optimized geometries.

The first ionization band observed in the photoelectron spectrum at 10.18 eV can be associated to the ionization process from the HOMO [$n\pi(S)$]. This orbital can be described as a lone pair formally localized on the sulfur atom. For example, the first vertical ionization energies for related species, such as FC(O)SCl,[45] ClC(O)SCl,[46] $ClC(O)SCH_3$,[15] $CH_3C(O)SH$,[47] $ClC(O)SCH_2CH_3$,[14] $CH_3C(O)SCH_2CH_3$[47] and $CH_3C(O)SCH_3$[48] are 10.68, 10.36, 10.11, 10.00, 9.84, 9.60 and 9.53 eV, respectively. The influence of the electronegativity of the atoms or groups bonding to the XC(O)SY skeleton becomes apparent.[49] Thus, higher HOMO ionization potentials are found for halogen substituted compounds (X= F and Cl), while the replacement by electron-releasing alkyl groups results in a decrease of the ionization potential (see Scheme 2). The low lying cation formed after HOMO ionization was further analyzed by quantum chemical calculations at the UB3LYP/6-311++G(d,p) level of approximation. In agreement with previous results,[45] the atomic charges are delocalized over the planar FC(O)S- fragment, with an appreciable fraction localized at the S atom, in qualitative agreement with the ionization of electrons from initially located in sulfur-type orbitals.

The second and third ionization bands observed in the photoelectron spectrum at 11.37 and 12.46 eV are assigned to the ionization process of an electron ejected from

the n_σ(O) and π(C=O) orbitals in the carbonyl group, respectively. The following lees-defined bands observed at 13.11 and 13.56 eV may be assigned to the ionization processes of the lone pair electrons located at fluorine atom, more specifically at the n_π and n_σ orbitals respectively.

It is significant to note that in the OVGF calculations included in the Gaussian03 package of programs, pole strengths larger than 0.80 are assumed to validate the one-electron picture of ionization.[50] Deleuze and coworkers show that pole strengths smaller than 0.85 corroborate a breakdown of the orbital picture of ionization.[51-55] Pole strengths larger than 0.85 were computed for the title species in the outermost valence electronic range.

Scheme 2. Energy of the HOMO [n_π(S)] for a series of related –SC(O)– compounds as determined from PES.

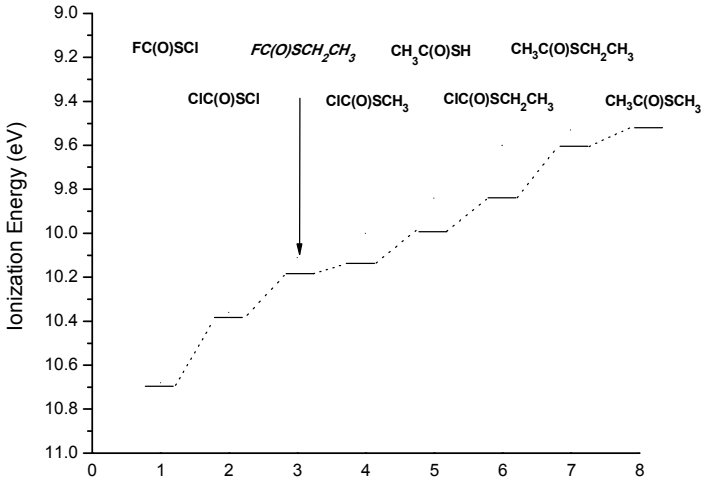

4.1.2-Photoionization and Photodissociation Processes in the Valence Region.

When the measurements were taken, the lowest photon energy achievable at the TGM beam line at the LNLS (11.10 eV) was higher than the first ionization potential of the $FC(O)SCH_2CH_3$ molecule (10.18 eV). Therefore, ionization processes are already

occurring at the very first step of the experiment. Figure 3 shows the PEPICO spectra recorded for $FC(O)SCH_2CH_3$ at selected photon energies. A fragment assignment of the signals is also given. The branching ratios for ion production are also listed in Table 2.

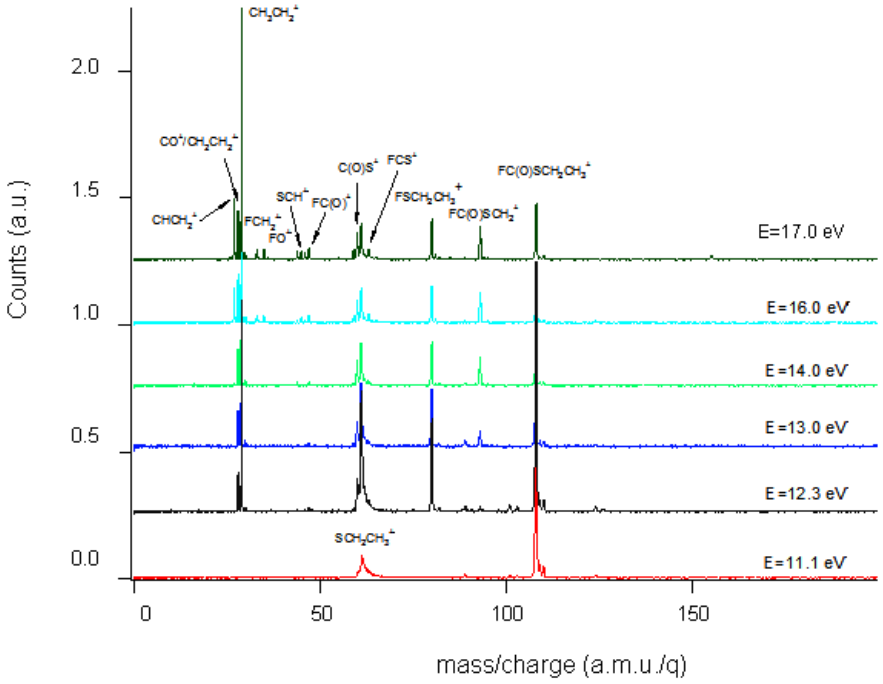

Figure 3. PEPICO spectra of $FC(O)SCH_2CH_3$ at different irradiation energies.

A very simple mass spectrum is obtained at 11.1 eV, with the presence of a signal at m/z= 108 assigned to the molecular ion accompanied by a second ion signal at 61 amu/q due to the $CH_3CH_2S^+$ species, probably originating from the α-rupture of the (O)C–S bond (loss of FC(O) fragment from molecular ion). When the energy of photons is increased, new ionization channels are opened. The $CH_3CH_2^+$ species is observed with high intensity at all measured energies in the valence region, reaching a contribution of up to ca. 38 % when the incident photon energy is 14.0 eV (See Table 2).

Interestingly, other of the most prominent dissociation channels in the valence region is the formation of the $CH_3CH_2SF^+$ cation, which occurs through an

intramolecular reorganization from the parent molecular ion. This decarbonylation process may involve the formation of β-distonic radical cations, as demonstrated for the case of $HC(O)SCH_2CH_3$.[10]

Table 2. Branching Ratios (%) for Fragment Ions Extracted from PEPICO Spectra Taken at Selected Photon Energies in the Valence Region of $FC(O)SCH_2CH_3$

m/z (amu/q))	Ion	Photon Energy (eV)					
		11.1	12.3	13.0	14.0	16.0	17.0
27	$C_2H_3^+$	-	-	-	-	6.2	8.9
28	$C_2H_4^+/CO^+$	-	4.7	6.4	6.6	7.1	7.1
29	$CH_3CH_2^+$	-	19.0	31.2	37.8	34.4	32.1
32	S^+	-	-	-	-	2.5	2.6
35	FO^+	-	-	-	-	2.0	2.5
44	CS^+	-	-	-	1.6	1.0	1.6
45	HCS^+	-	-	-	1.6	1.8	2.2
46	H_2CS^+	-	-	-	-	1.2	1.7
47	$FC(O)^+$	-	1.9	3.0	2.3	2.7	2.9
59	$C_2H_3S^+$	-	1.6	2.8	2.0	2.3	2.4
60	$C_2H_4S^+/OCS^+$	-	6.0	6.2	5.8	4.9	5.0
61	$CH_3CH_2S^+$	73.3	25.0	17.6	13.9	10.4	9.6
80	$FSCH_2CH_3^+$	-	11.3	10.8	9.2	7.3	6.7
93	$FC(O)SCH_2^+$	-	1.5	4.0	6.1	6.1	5.7
108	$FC(O)SCH_2CH_3^+$	26.7	28.8	17.8	13.0	9.9	8.9

The theoretical energy profile (TEP) has been computed at the UB3LYP/6-311++G(d,p) level of approximation to qualitatively analyze different ionization channels (Figure 4). The most probable theoretical dissociation channels that could occur in this range of energy are in very good agreement with the ions observed in the PEPICO TOF mass spectra. For example, the channel affording the $CH_3CH_2S^+$ ion and $FC(O)^{\cdot}$ radical is the energetically most favored, while the channel to form the $FC(O)^+$ ion appeared at higher energies. In the PEPICO spectrum at 11.1 eV only $CH_3CH_2S^+$

species is observed. The next photodissociation channel predicted from TEP is the formation of $CH_3CH_2SF^+$ cation discussed before, whereas the photodissociation channel involving the formation of CO^+ and $^{\cdot}FSCH_2CH_3$ requires more energy. In qualitative agreement with this finding, an intense signal at m/z= 80, due to the $CH_3CH_2SF^+$ ion, is observed in the PEPICOs obtained in the valence region.

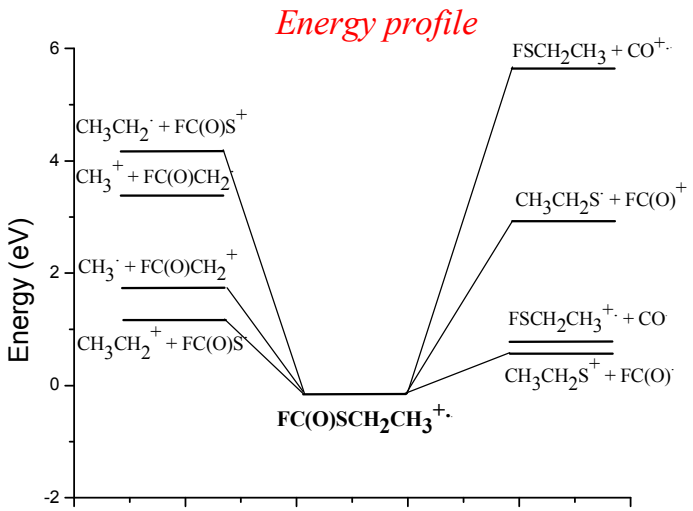

Figure 4. Theoretical Energy Profile for $FC(O)SCH_2CH_3$ computed at the UB3LYP/6-311++G(d,p) level of approximation.

4.2-Inner-shell S 2p and 2s electron region

To the best of our knowledge, the only core-shell electronic spectra available for thio- and (halo)thio-formate species are our recent works on the XC(O)SR (X= F, Cl and R= CH_3, CH_2CH_3) family of compounds, where the attention was paid especially at the S 2p electronic level, which was studied by acquiring the total ion yield (TIY) spectra, i.e. the count rate of the total ions as a function of the incident photon energy.[56] Double charged ions are expected to be produced after the core-shell ionization, mainly

due to Auger-type desexcitation processes. Thus, differences between the photoionization processes occurring in the valence and the inner shell regions are expected since they originate from different parent cations. In the following sections, the spectroscopic data as well as the dynamic of the ionic fragmentation at the S 2p level are analyzed. Special attention will be paid to determine whether the decarbonxylation process also occurred at higher photon energies or it is restricted to the outermost energy levels.

4.2.1-Total Ion Yield Spectra (TIY).

The TIY spectrum of $FC(O)SCH_2CH_3$ following S 2p excitations (from 162.0 to 174.0 eV photon energy) is shown in Figure 5. Below the S 2p threshold, a group of three signals centered at 164.0, 165.5 and 166.9 eV can be identified, while the ionization edge is located at approximately 171.4 eV. The signal centered at 229 eV can be assigned to the S 2s transition.

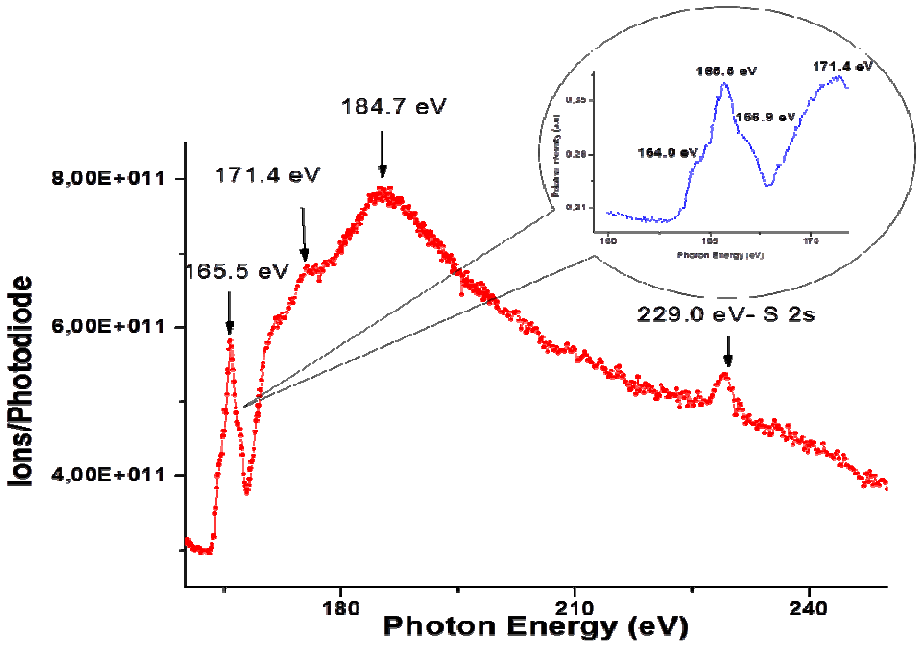

Figure 5. Total ion yield spectrum of $FC(O)SCH_2CH_3$ in the S 2p and S 2s regions.

Rather complex electronic processes can be anticipated at resonant energies below the S 2p ionization edge, which could be interpreted as dipole-allowed transitions that involve excitations of a 2p electron to antibonding molecular orbitals. The most abundant conformer of $FC(O)SCH_2CH_3$ belongs to the C_1 symmetry group and the dipole selection rules are totally relaxed in the transition processes. Quantum chemical calculations at the B3LYP/6-311++G(d,p) levels of approximation for neutral $FC(O)SCH_2CH_3$ in its ground state predict that these unoccupied orbitals should be mainly the LUMO $\pi^*_{C=O}$ and the σ^*_{S-C} and $\sigma^*_{S-C(O)}$ antibonding orbitals (See Figure 6).

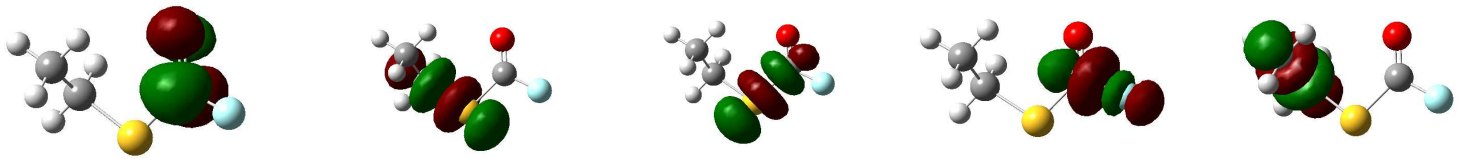

LUMO $\pi^*_{C=O}$ MO=29 | LUMO+1 (σ^*_{S-C}) MO=30 | LUMO+2 ($\sigma^*_{S-C(O)}$) MO=31 | LUMO+3 ($\sigma^*_{F-C(O)}$) MO=32 | LUMO+4 (σ^*_{C-C}) MO=33

Figure 6. Characters of the five lower energy unoccupied molecular orbitals for $FC(O)SCH_2CH_3$ calculated at the B3LYP/6-311++G(d,p) levels of approximation.

Previous photo-absorption measurements near the S 2p thresholds of –SC(O)– molecules,[10,48] yielded complicated spectra with rather undefined ionization edges preceded at lower energy by complex pattern of resonant transitions. The latter features were associated with transitions of the sulfur 2p electron into the lowest unoccupied molecular orbitals which are referred as "valence-shell states". Even for simple species, like H_2S, high-resolution measurements are necessary for the unambiguous assignment of these pre-edge transitions.[57] For the title species, the first absorption at 164.0 eV can be tentatively assigned to the S 2p → LUMO (π*C=O) transition, while the intense signal at 165.5 eV and the shoulder at 166.9 eV can be associated with dipole allowed transitions to the $\sigma^*_{S\text{-}C}$ and $\sigma^*_{S\text{-}C(O)}$ antibonding orbitals, respectively. Moreover, it is expected that a spin-orbital split occurs in the excited species for the 2p term of sulfur atom in $2p_{1/2}$ and $2p_{3/2}$ levels. For the simplest sulfide molecule, H_2S, this splitting was reported to be 1.201 eV.[57,58] Thus, it is plausible that the 165.5 and 169.9 eV signals also contain spin-orbital components. A similar spectral congestion was observed and in the analysis of the S 2p edge (by electron energy loss spectra[59] and total ion yield spectra[60]) for the simple CH_3SCN molecule.

4.2.2-PEPICO Spectra. Several PEPICO spectra have been recorded by setting the photon energy at each of the resonant values obtained in the TIY spectra, as well as at energies around 10 eV below and ca. 50 eV above the ionization edges for identifying the role of resonant processes in the fragmentation. PEPICO spectra at the resonance values observed in the S 2p edge (from the TIY spectrum) are shown in the Figure 7. After signal integration, the corresponding branching ratios were calculated for the main fragment ions and are gathered in Table 3. The signal at m/z= 108, corresponding to the molecular ion, is clearly observed through the whole range of energy. The most

abundant ion formed in both S 2p and S 2s energy range is $C_2H_3^+$ (10-16 % approximately), which may be formed due to the break of S-C simple bond from molecular ion with subsequent elimination of a H_2 molecule from $CH_2CH_3^+$ species. The last process has been studied in the ionic fragmentation of several species containing the ethyl group by different experimental techniques[61-64] and theoretical studies have also been performed.[65] The $C_2H_3^+$ ion, with m/z= 27, has also been observed as the most abundant ion in the investigations on $ClC(O)SCH_2CH_3$.[14]

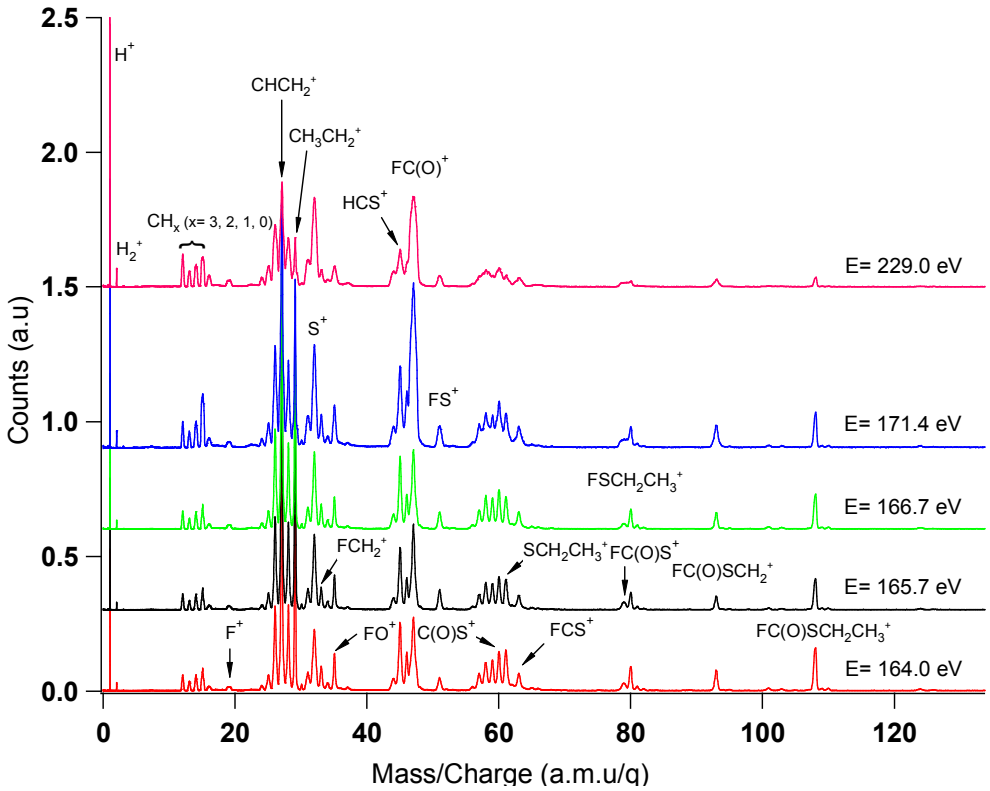

Figure 7. PEPICO spectra of $FC(O)SCH_2CH_3$ recorded at selected irradiation energies around S 2p and S 2s regions.

Other important signals in the spectra with relative abundances between 4 and 10 % are: H^+ (m/z= 1), $CH_2CH_2^+/CO^+$ (m/z= 28), $CH_2CH_3^+$ (m/z= 29), S^+ (m/z= 32), HCS^+ (m/z= 45) and $FC(O)^+$ (m/z= 47). The stability of the fragment HCS^+ has been

already stressed and linked with its abundance as an important interstellar species.[42] Finally, the description of the spectra is complemented by the presence of the following less abundant fragments: the methyl fragments, CH_x^+ (x=0, 1, 2, 3), with m/z= 12, 13, 14 and 15, O^+ or S^{+2} (m/z= 16), FCH_x^+(x=0, 1, 2) with m/z= 31, 32 and 33, FO^+(m/z= 35), H_xCS (x= 0, 2) with m/z= 44 and 46, FS^+(m/z= 51), $C_2H_xS^+$ (x= 0, 1, 2, 3, 4, 5) with m/z= 56, 57, 58, 59, 60 and 61, FCS^+ (m/z= 63), $FSCH_2CH_3^+$(m/z= 80) and $FC(O)SCH_2^+$(m/z= 93).

Table 3. Branching Ratios (%) for Fragment Ions Extracted from PEPICO Spectra Taken at a Photon Energy around S 2p and S 2s Energies for $FC(O)SCH_2CH_3$. Kinetic Energy Release Values (eV) are Given for Selected Photon Energies (165.7, 171.4 and 229.0 eV).

		Photon energy (eV)						
		Off resonance	**S 2p**				**Off resonance**	**S 2s**
m/z	**Ion**	**155.0**	**164.0**	**165.7** [a]	**166.7**	**171.4**	**210.0**	**229.0** [a]
1	H^+	5.56	5.45	5.18/*3.81*	5.80	6.73/*4.70*	9.58	10.6/*5.80*
2	H_2^+	0.47	0.47	0.46	0.49	0.64/*5.80*	0.95	1.00/*6.89*
12	C^+	1.24	1.30	1.38/*2.60*	1.41	1.34/*2.37*	2.21	2.60/*3.23*
13	CH^+	0.86	0.85	0.84/*2.37*	0.90	0.95/*2.87*	1.28	1.42/*3.57*
14	CH_2^+	1.42	1.43	1.43/*2.67*	1.50	1.75/*3.75*	2.25	2.29/*4.75*
15	CH_3^+	2.06	2.01	1.90/*2.60*	2.00	3.82/*4.19*	3.80	3.29/*4.66*
16	O^+	0.71	0.70	0.71/*5.77*	0.73	0.97/*6.20*	1.22	1.37/*5.01*
19	F^+	0.79	0.74	0.75	0.75	0.76/*7.13*	0.95	1.04/*8.00*
24	CC^+	0.60	0.59	0.58	0.62	0.67	0.91	0.97
25	C_2H^+	1.49	1.52	1.57/*0.86*	1.66	1.62/*1.55*	2.14	2.23/*2.07*
26	$C_2H_2^+$	6.13	6.53	7.21/*0.99*	7.33	6.09/*2.28*	6.88	6.93/*3.22*
27	$C_2H_3^+$	14.39	15.28	15.98/*0.48*	15.20	12.2/*1.25*	10.8	9.74/*2.24*
28	$C_2H_4^+/CO^+$	5.27	5.56	6.17/*0.70*	5.65	4.47/*1.62*	5.07	5.08/*2.87*
29	$CH_3CH_2^+$	9.79	9.20	9.24/*0.20*	8.17	5.52/*0.27*	3.79	3.26/*0.76*
31	FC^+	1.63	1.83	2.01/*1.00*	2.03	2.28/*2.03*	3.08	3.08/*2.46*
32	S^+/FCH^+	5.61	6.14	7.14/*1.28*	6.88	6.74/*1.74*	9.76	10.2/*2.75*
33	FCH_2^+	1.89	1.81	1.67/*0.43*	1.76	1.74/*0.88*	1.68	1.60/*1.10*
35	FO^+	2.20	2.29	2.16/*0.25*	2.01	2.25/*0.88*	2.69	2.09/*2.13*
44	CS^+	1.30	1.25	1.23/*1.56*	1.39	1.41/*1.83*	1.67	1.58/*1.11*
45	HCS^+	5.16	5.20	4.80/*0.52*	5.24	4.79/*0.97*	4.61	3.82/*3.32*

46	H_2CS^+	2.44	2.33	2.03/*0.65*	2.12	2.53/*0.58*	[b]	1.88
47	$FC(O)^+$	7.33	7.74	8.09/*0.93*	7.82	13.9/*2.55*	16.51	12.9/*3.67*
51	FS^+	0.96	1.13	1.63/*0.45*	1.38	1.47/*0.92*	1.29	1.10/*1.03*
56	C_2S^+	0.43	0.40	0.38/	0.42	0.41	[b]	0.29
57	$C2HS^+$	1.48	1.44	1.32/*0.58*	1.53	1.37/*1.57*	[b]	1.05
58	$C_2H_2S^+$	2.21	2.25	2.07/*0.44*	2.41	2.06/*0.73*	[b]	1.69
59	$C_2H_3S^+$	2.17	2.07	1.88/*0.40*	2.05	1.71/*1.11*	[b]	1.12
60	$C_2H_4S^+/OCS^+$	3.06	2.64	2.30/*0.36*	2.62	2.51/*0.71*	2.40	1.72/*1.38*
61	$CH_3CH_2S^+$	3.45	3.09	2.42/*0.42*	2.45	2.05/*0.95*	1.31	1.15/*1.07*
63	FCS^+	1.75	1.52	1.36/*0.68*	1.50	1.42/*1.73*	1.32	1.01/*1.71*
79	$FC(O)S^+$	0.44	0.75	0.78/*0.51*	0.57	0.75	[b]	0.50
80	$FSCH_2CH_3^+$	1.57	1.25	0.92/*0.10*	1.01	0.80/*0.12*	0.42	0.38
93	$FC(O)SCH_2^+$	1.59	1.19	0.86/*0.10*	0.97	1.14/*0.27*	0.80	0.60/*0.42*
108	$FC(O)SCH_2CH_3^+$	2.57	2.07	1.54/*0.07*	1.65	1.07/*0.07*	0.55	0.43/*0.08*

[a] Kinetic energy release values determined at selected energies are given in italics. [b] Overlapping of peaks is observed.

It is important to note that many of these fragments contain the fluorine atom, and under unimolecular condition, it should be formed from internal recombination processes within the molecule after ionization. For example, FO^+ and FS^+ are clearly observed in the spectra, reaching branching values of 2.16 and 1.63 % at 165.7 eV, respectively. The FS^+ ion can be formed by ethyl elimination after the decarbonylation process, as is shown in Scheme 3. It is well-known that at energies below the ionization of core electrons, Auger Participator decay (characterized by excitation of core electrons to virtual molecular orbitals) can produces relatively long-lived one-hole valence final states.[66]

Scheme 3. Decarbonylation process following ethyl elimination of $FC(O)SCH_2CH_3$ molecule.

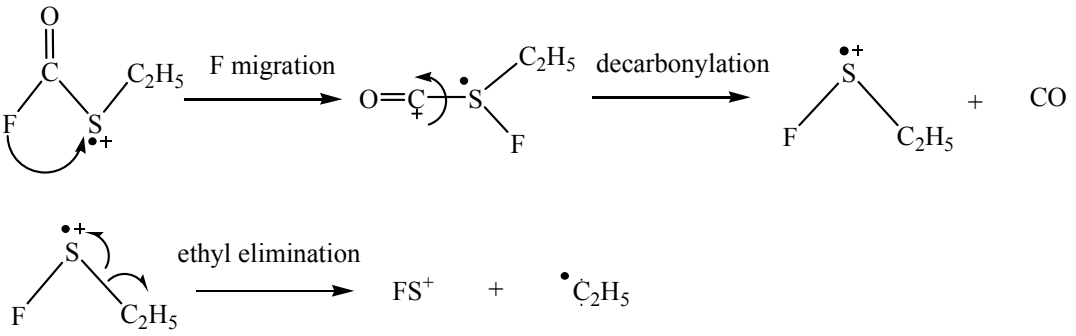

From the full width at half maximum of the signals observed in the PEPICO, the kinetic energy release (KER) value has been determined for each ion, as listed in Table 3 for selected photon energies. Much higher KER values are clearly observed for the spectra above the S 2p edge (171.4 eV) and in the S 2s region, in agreement with the occurrence of normal Auger decay of core-shell-excited species. In the present case, a double valence-hole final state is expected, leading to the formation of doubly charged

parent ions, which dissociate releasing much of their internal energy as kinetic energy of the fragment ions (KER).

As showed below, after S 2p excitations the PEPICO spectra have contribution of both single and double ionization processes. The heaviest fragments detected, $FC(O)SCH_2^+$ and $FSCH_2CH_3$ ions, must be only produced from the singly charged species $FC(O)SCH_2CH_3^{\cdot+}$. The peak shape corresponding to these ions are sharp and symmetric with small variations on the KER values (See Table 3).

Another ion observed with relative low KER values in the whole energy range is the $CH_3CH_2^+$ fragment, which involves the rupture of the S-C bond. Because of the low ionization potential for the CH_2CH_3 radical,[61-64] the charge is retained on this fragment and the $FC(O)S^+$ cation is not detected in the PEPICO spectra. The following simple mechanism explain the experimental observation:

$$FC(O)SCH_2CH_3^{\bullet+} \rightarrow CH_2CH_3^+ + FC(O)S^{\bullet} \text{ (KER= 0.20-0.76 eV)}$$

As commented before, the $M^{\cdot+}$ molecular ion is observed in the whole range of photon energies studied with a KER close to the "thermal" value of 0.05 eV, as expected.[29] The observation of the singly charged molecular ion reinforces the important role of Participator Auger processes in the electronic decay of the excited species below the S 2p ionization thresholds.

4.2.3-PEPIPICO Spectra.

Two-dimensional PEPIPICO spectra were recorded at each of the resonant energies values on the S 2p and S 2s regions. The analysis of the shape and slope of the coincidence islands appearing in the PEPIPICO spectra bring important information for identifying two-, three-[21] and four-body dissociation mechanisms for ionic fragmentation.

Coincidence between ions with m/z values of 27 amu/q ($C_2H_3^+$) and 51 amu/q (FS^+). This coincidence is observed in the PEPIPICOs as well-defined and intense islands, as can be observed in Figure 8 for the spectrum at 165.7 eV. Plausible mechanisms should include an internal recombination involving the migration of fluorine atom from carbonyl group to sulfur atom. The shape and slope (–0.73) displayed by this coincidence are in agreement with the occurrence of the four-body Secondary Decay in Competition (SDC) mechanism delineated as follow:

$FC(O)SCH_2CH_3^{2+} \rightarrow FC(O)S^+ + CH_2CH_3^+$

$FC(O)S^+ \rightarrow FS^+ + CO$ $\alpha^{calc} = -0.69$

$CH_2CH_3^+ \rightarrow C_2H_3^+ + H_2$

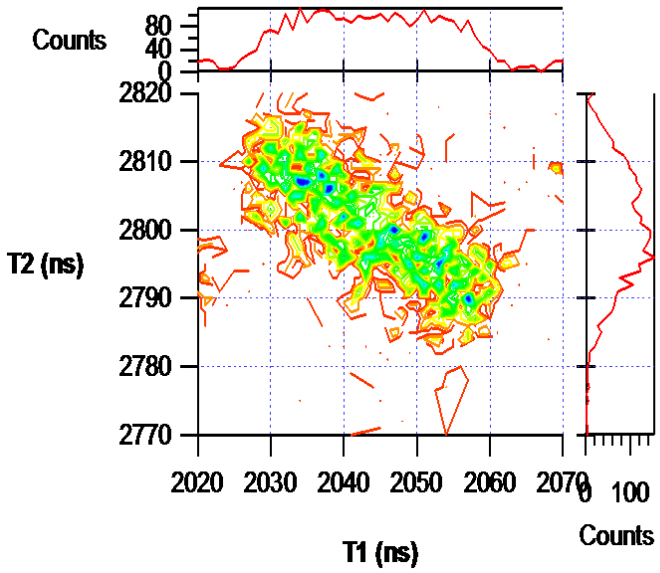

Figure 8. Contour plot for the coincidence island between $C_2H_3^+$ (T1) and FS^+ (T2) ions derived from 165.7 eV PEPIPICO spectrum of $FC(O)SCH_2CH_3$.

Coincidence between ions with m/z values of 27 amu/q ($C_2H_3^+$) and 32 amu/q (S^+). This coincidence is the most intense island appearing along the S 2p region, observed as a well-defined parallelogram with a slope of –0.87 (see Figure 9). Several mechanisms could be proposed to explain the appearance of this couple of ions in coincidence; however the experimental shape and slope are better interpreted by the occurrence of the deferred charge separation (DCS) mechanism delineated as follow:

$$FC(O)SCH_2CH_3^{2+} \rightarrow FC(O)SC_2H_3^{2+} + H_2$$

$$FC(O)SC_2H_3^{2+} \rightarrow FC(O) + SC_2H_3^{+2} \qquad \alpha^{calc} = -1.0$$

$$SC_2H_3^{+2} \rightarrow S^+ + C_2H_3^+$$

The expected slope for the $C_2H_3^+/S^+$ island is equal to –1, a value which is higher than the experimental one. The occurrence of other dissociative mechanisms acting in competition can not be ruled out.

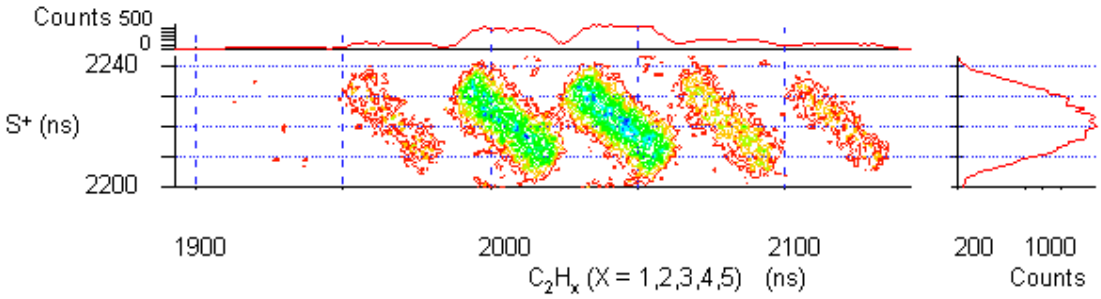

Figure 9. Contour plot for the coincidence island between $C_2H_x^+$ (T1) and S^+ (T2) ions derived from 165.7 eV PEPIPICO spectrum of $FC(O)SCH_2CH_3$.

Coincidence between ions with m/z values of 27 amu/q ($C_2H_3^+$) and 60 amu/q (OCS^+). The four-body Secondary Decay in Competition (SDC) represents a plausible mechanism for this coincidence. The calculated slope is –0.80 according to SDC, if the kinetic energy release corresponding to the neutral ejection is neglected. This value is in very good agreement with the experimental one (–0.84), as shown in figure 10.

$FC(O)SCH_2CH_3^{2+} \rightarrow FC(O)S^+ + CH_2CH_3^+$

$FC(O)S^+ \rightarrow OCS^+ + F$ $\qquad \alpha^{calc} = -0.80$

$CH_2CH_3^+ \rightarrow C_2H_3^+ + H_2$

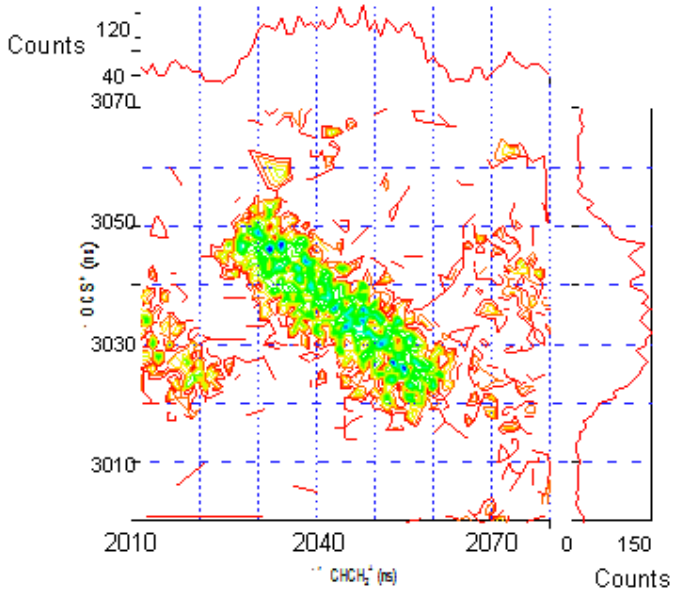

Figure 10. Contour plot for the coincidence island between $C_2H_3^+$ (T1) and OCS^+ (T2) ions derived from 165.7 eV PEPIPICO spectrum of $FC(O)SCH_2CH_3$.

5-Conclusions

The PES spectrum of $FC(O)SCH_2CH_3$ was analyzed and the valence electronic structure determined. The three first ionization bands appearing in the spectrum at 10.18 11.37 and 12.46 eV are associated with ionization processes of electrons formally located on the –SC(O)– group [$n\pi(S)$, $n_\sigma(O)$ and $\pi(C=O)$ orbitals, respectively].

The joint application of time-of-flight mass spectrometry (in the PEPICO and PEPIPICO modes) and synchrotron radiation as monochromatic photon source allowed a detailed study of the ionic fragmentation of the $FC(O)SCH_2CH_3$ molecule in the gas phase following valence and shallow-core (S 2p and 2s) excitations. Dissociation mechanisms have been proposed in order to explain the ionic fragmentation decay for singly- and double-charged excited species. In the valence region the PEPICO spectra at different energies can be interpreted straightforwardly. The $CH_3CH_2^+$ species is

observed with high intensities at all measured energies in agreement with the dissociation channels proposed for the photoevolution of the title molecule.

A group of three signals centered at 164.0, 165.5 and 166.9 eV in the TIY spectrum of $FC(O)SCH_2CH_3$ can be interpreted as due to resonant transitions corresponding to dipole-allowed transitions involving excitations of a 2p electron to an antibonding molecular orbital. In this energy range, $C_2H_3^+$ (10-16 % approximately) is the most abundant ion, which may be produced due to the excision of S-C simple bond from the molecular ion with the subsequent elimination of a H_2 molecule from $CH_2CH_3^+$ species.

The analysis of the PEPIPICO spectra has been used to identify the dissociation mechanisms for doubly charged parent ions. The observation of the FS^+ ion in these spectra confirms that molecular rearrangements also occurred on highly charged species.

Supporting information: ^1H NMR and ^{19}F NMR of $FC(O)SCH_2CH_3$ and vibrational spectra (IR(gas), Raman (liquid). Calculated relative energies for stable conformers of $FC(O)SCH_2CH_3$ in the ground (in kcal mol^{-1}) electronic states .This information is available free of charge via the Internet at http://pubs.acs.org.

6- Acknowledgment

This work has been largely supported by the Brazilian Synchrotron Light Source (LNLS). The authors wish to thank Arnaldo Naves de Brito and his research group for fruitful discussions and generous collaboration during their several stays in Campinas and the TGM beam line staffs for their assistance throughout the experiments. They also

are indebt to the Agencia Nacional de Promoción Científica y Tecnológica (ANPCyT), Consejo Nacional de Investigaciones Científicas y Técnicas (CONICET), and the Facultad de Ciencias Exactas, Universidad Nacional de La Plata for financial support. CODV, MFE and RMR acknowledge the support of the Chinese Academy of Sciences to work in the Institute of Chemistry of the Chinese Academy of Science in Beijing.

References

(1) Bodi, A.; Hemberger, P.; Osborn, D. L.; Sztáray, B. Mass-Resolved Isomer-Selective Chemical Analysis with Imaging Photoelectron Photoion Coincidence Spectroscopy. *J. Phys. Chem. Lett.* **2013**, *4*, 2948-2952.

(2) Harvey, J.; Tuckett, R. P.; Bodi, A. A Halomethane Thermochemical Network from iPEPICO Experiments and Quantum Chemical Calculations. *J. Phys. Chem. A* **2012**, *116*, 9696-9705.

(3) Shin, J.-W.; Bernstein, E. R. Vacuum Ultraviolet Photoionization of Carbohydrates and Nucleotides. *J. Chem. Phys.* **2014**, *140*, 44330-44339.

(4) Itälä, E.; Huels, M. A.; Rachlew, E.; Kooser, K.; Hägerth, T.; Kukk, E. A Comparative Study of Dissociation of Thymidine Molecules Following Valence or Core Photoionization. *J. Phys. B* **2013**, *46*, 215102.

(5) Weng, J.; Jia, L.; Wang, Y.; Sun, S.; Tang, X.; Zhou, Z.; Kohse-Häinghaus, K.; Qi, F. Pyrolysis Study of Poplar Biomass by Tunable Synchrotron Vacuum Ultraviolet Photoionization Mass Spectrometry. *Proc. Comb. Instit.* **2013**, *34*, 2347-2354.

(6) Alligood, B. W.; Womack, C. C.; Brynteson, M. D.; Butler, L. J. Dissociative Photoionization of $CH_3C(O)CH_2$ to $C_2H_5^+$. *Int. J. Mass Spectrom.* **2011**, *304*, 45-50.

(7) Moreno Betancourt, A.; Flores Antognini, A.; Erben, M. F.; Cavasso-Filho, R.; Tong, S.; Ge, M.; Della Védova, C. O.; Romano, R. M. Electronic Properties of Fluorosulfonyl Isocyanate, FSO_2NCO: A Photoelectron Spectroscopy and Synchrotron Photoionization Study. *J. Phys. Chem. A* **2013**, *117*, 9179-9188.

(8) Gomes, A. H. A.; Wolff, W.; Ferreira, N.; Alcantara, K. F.; Luna, H.; Sigaud, G. M.; Santos, A. C. F. Deep Core Ionic Photofragmentation of the CF_2Cl_2 Molecule. *Int. J. Mass Spectrom.* **2012**, *319-320*, 1-8.

(9) Le, H. T.; Nguyen, T. L.; Lahem, D.; Flammang, R.; Nguyen, M. T. Potential Energy Surfaces Related to Thioxy-hydroxy-carbene (HSCOH) and its Radical Cation. *Phys. Chem. Chem. Phys.* **1999**, *1*, 755 - 760.

(10) Flammang, R.; Lahem, D.; Nguyen, M. T. Novel β-Distonic Radical Cations $[C_nH_{2n+2}S]^{\cdot+}$ (n = 2, 3) Formed upon Decarbonylation of Ionized S-Alkyl Thioformates: A Mass Spectrometric and ab Initio Study. *J. Phys. Chem. A* **1997**, *101*, 9818-9823.

(11) Flammang, R.; Nguyen, M. T.; Bouchoux, G.; Gerbaux, P. Characterization of Ionized Carbenes in the Gas Phase. *Int. J. Mass Spectrom.* **2000**, *202*, A8-A25.

(12) Bouma, W. J.; Nobes, R. H.; Radom, L. Unusual Low-Energy Isomers of the Ethanol and Dimethyl Ether Radical Cations. *J. Am. Chem. Soc.* **1983**, *105*, 1743-1746.

(13) Bouchoux, G.; Berruyer, F.; Hiberty, P. C.; Wu, W. Classical and Distonic Radical Cations: A Valence Bond Approach. *Chem. Eur. J.* **2007**, *13*, 2912-2919.

(14) Rodríguez Pirani, L. S.; Erben, M. F.; Geronés, M.; Ma, C.; Ge, M.; Romano, R. M.; Cavasso Filho, R. L.; Della Védova, C. O. Outermost and Inner-Shell Electronic Properties of $ClC(O)SCH_2CH_3$ Studied Using HeI Photoelectron Spectroscopy and Synchrotron Radiation. *J. Phys. Chem. A* **2011**, *115*, 5307-5318.

(15) Geronés, M.; Erben, M. F.; Ge, M.; Cavasso Filho, R. L.; Romano, R. M.; Della Védova, C. O. Study of the Photodissociation Process of $ClC(O)SCH_3$ Using

both Synchrotron Radiation and HeI Photoelectron Spectroscopy in the Valence Region. *J. Phys. Chem. A* **2010**, *114*, 8049-8055.

(16) Geronés, M.; Erben, M. F.; Romano, R. M.; Cavasso Filho, R. L.; Della Védova, C. O. Evidence for the Formation of an Interstellar Species, HCS^+, during the Ionic Fragmentation of Methyl Thiofluoroformate, $FC(O)SCH_3$, in the 100-1000 eV Region. *J. Phys. Chem. A* **2010**, *114*, 12353-12361.

(17) Geronés, M.; Erben, M. F.; Romano, R. M.; Cavasso Filho, R. L.; Della Védova, C. O. Dissociative Photoionization of Methyl Thiochloroformate, $ClC(O)SCH_3$, Following Sulfur 2p, Chlorine 2p, Carbon 1s, and Oxygen 1s Excitations. *J. Phys. Chem. A* **2012**, *116*, 7498-7507.

(18) Lira, A. C.; Rodrigues, A. R. D.; Rosa, A.; Gonçalves da Silva, C. E. T.; Pardine, C.; Scorzato, C.; Wisnivesky, D.; Rafael, F.; Franco, G. S.; Tosin, G.; et. al. "First Year Operation of the Brazilian Synchrotron Light Source"; European Particle Accelerator Conference, 1998, Stockholm.

(19) de Fonseca, P. T.; Pacheco, J. G.; Samogin, E.; de Castro, A. R. B. Vacuum ultraviolet beam lines at Laboratório Nacional de Luz Síncrotron, the Brazilian Synchrotron Source. *Rev. Sci. Instr.* **1992**, *63*, 1256-1259.

(20) Kivimaki, A.; Ruiz, J. A.; Erman, P.; Hatherly, P.; Garcia, E. M.; Rachlew, E.; Riu, J. R. i.; Stankiewicz, M. An Energy Resolved Electron-Ion Coincidence Study Near the S 2p Thresholds of the SF_6 Molecule. *J. Phys. B: At. Mol. Opt. Phys.* **2003**, 781-791.

(21) Frasinski, L. J.; Stankiewicz, M.; Randall, K. J.; Hatherly, P. A.; Codling, K. Dissociative Photoionisation of Molecules Probed by Triple Coincidence; Double Time-of-Flight Techniques. *J. Phys. B: At. Mol. Phys.* **1986**, *19*, L819-L824.

(22) Eland, J. H. D.; Wort, F. S.; Royds, R. N. A Photoelectron-Ion-Ion Triple Coincidence Technique for the Study of Double Photoionization and its Consequences *J. Electron Spectrosc. Rel. Phenom.* **1986**, *41*, 297-309.

(23) Naves de Brito, A.; Feifel, R.; Mocellin, A.; Machado, A. B.; Sundin, S.; Hjelte, I.; Sorensen, S. L.; Bjorneholm, O. Femtosecond Dissociation Dynamics of Core-Excited Molecular Water. *Chem. Phys. Lett.* **1999**, *309*, 377-385.

(24) Cavasso Filho, R. L.; Homem, M. G. P.; Landers, R.; Naves de Brito, A. Advances on the Brazilian Toroidal Grating Monochromator (TGM) Beamline. *J. Electron Spectrosc. Rel. Phenom.* **2005**, *144-147*, 1125-1127.

(25) Filho, R. L. C.; Lago, A. F.; Homem, M. G. P.; Pilling, S.; Brito, A. N. d. Delivering High-Purity Vacuum Ultraviolet Photons at the Brazilian Toroidal Grating Monochromator (TGM) Beamline *J. Electron Spectrosc. Relat. Phenom.* **2007**, *156-158*, 168-171

(26) Cavasso Filho, R.; Homem, M. G. P.; Fonseca, P. T.; Naves de Brito, A. A Synchrotron Beamline for Delivering High Purity Vacuum Ultraviolet Photons. *Rev. Sci. Instr.* **2007**, *78*, 115104-115108.

(27) Laskin, J.; Lifshitz, C. Kinetic Energy Release Distributions in Mass Spectrometry. *J. Mass Spectrom.* **2001**, *36*, 459-478.

(28) Pilling, S.; Lago, A. F.; Coutinho, L. H.; de Castilho, R. B.; de Souza, G. G. B.; Naves de Brito, A. Dissociative Photoionization of Adenine Following Valence Excitation. *Rapid Commu. Mass Spectrom.* **2007**, *21*, 3646-3652.

(29) Santos, A. C. F.; Lucas, C. A.; de Souza, G. G. B. Dissociative Photoionization of SiF_4 Around the Si 2p Edge: A New TOFMS Study with Improved Mass Resolution. *J. Electron Spectrosc. Rel. Phenom.* **2001**, *114-116*, 115-121.

(30) Huang, W. C.; Lin, Y. C.; Tzeng, W. B. Mass-Analyzed Threshold Ionization Spectroscopy of 2,6-Dimethylaniline, 2,6-Dimethylaniline-NHD, and 2,6-Dimethylaniline-ND2. *Chem. Phys. Lett.* **2012**, *551*, 50-53.

(31) Yao, L.; Zeng, X. Q.; Ge, M. F.; Wang, W. G.; Sun, Z.; Du, L.; Wang, D. X. First Experimental Observation of Gas-Phase Nitrosyl Thiocyanate. *Eur. J. Inorg. Chem.* **2006**, 2469-2475.

(32) Xiaoqing, Z.; Fengyi, L.; Qiao, S.; Ge, M.; Jianping, Z.; Xicheng, A.; Lingpeng, M.; Shijun, Z.; Dianxun, W. Reaction of AgN_3 with $SOCl_2$: Evidence for the Formation of Thionyl Azide, $SO(N_3)_2$. *Inorg. Chem.* **2004**, *43*, 4799-4801.

(33) Wang, W.; Yao, L.; Zeng, X.; Ge, M.; Sun, Z.; Wang, D.; Ding, Y. Evidence of the Formation and Conversion of Unstable Thionyl Isocyanate: Gas-Phase Spectroscopic Studies. *J. Chem. Phys.* **2006**, *125*, 234303.

(34) Li, Y.; Zeng, X.; Sun, Q.; Li, H.; Ge, M.; Wang, D. Electronic Structure of H_2CS_3 and H_2CS_4: An Experimental and Theoretical Study. *Spectrochim. Acta Part A: Molec. Biomolec. Spectroscopy* **2007**, *66*, 1261-1266.

(35) Zhao, H. Q.; Wang, D. X.; Xu, G. Z. *J. Anal. Instrum.* **1992**, 4, 23.

(36) Tarantelli, F.; Cederbaum, L. S. Foreign Imaging in Auger Spectroscopy: The Si 2p Spectrum of Silicon Tetrafluoride. *Phys. Rev. Lett.* **1993**, *71*, 649.

(37) DeFrees, D. J.; Binkley, J. S.; Frisch, M. J.; McLean, A. D. Is N-Protonated Hydrogen Isocyanide, H_2NC^+, an Observable Interstellar Species?. *J. Chem. Phys.* **1986**, *85*, 5194-5199.

(38) Salomon, C. J.; Breuer, E. Facile "One-Pot" Preparation of Phosphonothiolformates. Useful Reagents for the Synthesis of Carbamoylphosphonates. *SynLett.* **2000**, *6*, 0815-0816.

(39) Ulic, S. E.; Coyanis, E. M.; Romano, R. M.; Della Védova, C. O. S-Ethyl Thiochloroformate, $ClC(O)SCH_2CH_3$: Unusual Conformational Properties? *Spectrochim. Acta* **1998**, *A54*, 695-705.

(40) Deleuze, M. S.; Pang, W. N.; Salam, A.; Shang, R. C. Probing Molecular Conformations with Electron Momentum Spectroscopy: The Case of n-Butane. *J. Am. Chem. Soc.* **2001**, *123*, 4049-4061.

(41) Deleuze, M. S.; Knippenberg, S. Study of the Molecular Structure, Ionization Spectrum, and Electronic Wave Function of 1,3-Butadiene Using Electron Momentum Spectroscopy and Benchmark Dyson Orbital Theories. *J. Chem. Phys.* **2006**, *125*, 104309.

(42) Morini, F.; Knippenberg, S.; Deleuze, M. S.; Hajgato, B. Quantum Chemical Study of Conformational Fingerprints in the Photoelectron Spectra and (e, 2e) Electron Momentum Distributions of n-Hexane. *J. Phys. Chem. A* **2010**, *114*, 4400-4417.

(43) True, N. S.; Clarence, J. S.; Bohn, R. K.; J., S. Low Resolution Microwave Spectroscopy. 12. Conformations and Approximate Barriers to Internal Rotation in Ethyl Thioesters. *J. Phys. Chem.* **1981**, *85*, 1132-1137.

(44) Turchaninov, V. K.; Chipanina, N. N.; Aksamentova, T. N.; Sorokin, M. S.; Pestunovich, V. A. AM1 Studies of Photoelectron Spectra. *Russ. Chem. Bull.* **1998**, *47*, 231-236.

(45) Erben, M. F.; Della Védova, C. O. Dramatic Changes in Geometry after Ionization: Experimental and Theoretical Studies on the Electronic Properties of Fluorocarbonyl (Mono-, Di-, and Tri-) Sulfur Compounds. *Inorg. Chem.* **2002**, *41*, 3740-3748.

(46) Gerones, M.; Erben, M. F.; Romano, R. M.; Della Védova, C. O.; Yao, L.; Ge, M. He I Photoelectron Spectra and Valence Synchrotron Photoionization for XC(O)SCl (X = F, Cl) Compounds. *J. Phys. Chem. A* **2008**, *112*, 2228-2234.

(47) Nagata, S.; Yamabe, T.; Fukui, K. Electronic Spectra of Thioacetic Acid and its Ethyl Ester. *J. Phys. Chem.* **1975**, *79*, 2335-2340.

(48) Geronés, M.; Downs, A. J.; Erben, M. F.; Ge, M.; Romano, R. M.; Yao, L.; Della Védova, C. O. HeI Photoelectron and Valence Synchrotron Photoionization Studies of the Thioester Molecule $CH_3C(O)SCH_3$: Evidence of Vibronic Structure. *J. Phys. Chem. A* **2008**, *112*, 5947-5953.

(49) Dezarnaud-Dandine, C.; Bournel, F.; Mangeney, C.; Tronc, M.; Modelli, A.; Jones, D. Empty Levels Probed by XAS and ETS in Cyclic Polymethylene Sulfides $(CH_2)_nS$, n=2, 3, 4, 5. *Chem. Phys.* **2001**, *265*, 105-112.

(50) Zakrzewski, V. G.; Ortiz, J. V.; Nichols, J. A.; Heryadi, D.; Yeager, D. L.; Golab, J. T. Comparison of Perturbative and Multiconfigurational Electron Propagator Methods. *Int. J. Quantum Chem.* **1996**, *60*, 29-36.

(51) Deleuze, M. S. Valence One-Electron and Shake-Up Ionization Bands of Polycyclic Aromatic Hydrocarbons. II. Azulene, Phenanthrene, Pyrene, Chrysene, Triphenylene, and Perylene. *J. Chem. Phys.* **2002**, *116*, 7012-7026.

(52) Knippenberg, S.; Nixon, K. L.; Brunger, M. J.; Maddern, T.; Campbell, L.; Trout, N.; Wang, F.; Newell, W. R.; Deleuze, M. S.; Francois, J. P. et al. An Investigation into its Valence Electronic Structure using Electron Momentum Spectroscopy, and Density Functional and Green's Function Theories. *J. Chem. Phys.* **2004**, *121*, 10525-10541..

(53) Deleuze, M. S. Valence One-Electron and Shake-Up Ionization Bands of Polycyclic Aromatic Hydrocarbons. III. Coronene, 1.2,6.7-Dibenzopyrene, 1.12-Benzoperylene, Anthanthrene. *J. Phys. Chem. A* **2004**, *108*, 9244-9259.

(54) Kishimoto, N.; Hagihara, Y.; Ohno, K.; Knippenberg, S.; Francois, J.-P.; Deleuze, M. S. Probing the Shape and Stereochemistry of Molecular Orbitals in Locally Flexible Aromatic Chains: A Penning Ionization Electron Spectroscopy and Green's Function Study of the Electronic Structure of Biphenyl. *J. Phys. Chem. A* **2005**, *109*, 10535-10546.

(55) Deleuze, M. S. Valence One-Electron and Shake-Up Ionisation Bands of Polycyclic Aromatic Hydrocarbons. IV. The Dibenzanthracene Species. *Chem. Phys.* **2006**, *329*, 22-38.

(56) Nenner, I.; Beswick, J. A. Molecular Photodissociation and Photoionization. In *Handbook on Synchrotron Radiation*; Marr, G. V., Ed.; Elsevier Science Publishers: Amsterdam, 1987; Vol. 2; pp 355-462.

(57) Hudson, E.; Shirley, D. A.; Domke, M.; Remmers, G.; Kaindl, G. High-Resolution Photoabsorption Near the Sulfur $L_{2,3}$ Thresholds: H_2S and D_2S. *Phys. Rev. A* **1994**, *49*, 161-175.

(58) Svensson, S.; Naves de Brito, A.; Keane, M. P.; Correia, N.; Karlsson, L. Observation of an Energy Shift in the $S2p_{3/2}$–$S2p_{1/2}$ Spin-Orbit Splitting between X-Ray Photoelectron and Auger-Electron Spectra for the H_2S Molecule. *Phys. Rev. A* **1991**, *43*, 6441–6443.

(59) Hitchcock, A. P.; Tronc, M.; Modelli, A. Electron Transmission and Inner-Shell Electron Energy Loss Spectroscopy of Acetonitrile, Isocyanomethane, Methyl Thiocyanate, and Isothiocyanatomethane. *J. Phys. Chem.* **1989**, *93*, 3068-3077.

(60) Cortés, E.; Erben, M. F.; Geronés, M.; Romano, R. M.; Della Védova, C. O. Dissociative Photoionization of Methyl Thiocyanate, CH_3SCN, in the Proximity of the Sulfur 2p Edge. *J. Phys. Chem. A* **2009**, *113*, 564-572.

(61) Dudley H. Williams, G. H. Kinetic Energy Release in Relation to Symmetry-Forbidden Reactions. *J. Am. Chem. Soc.* **1974**, *96*, 6753–6755.

(62) Williams, D. H.; Hvistendahl, G. Kinetic Energy Release as a Mechanistic Probe. Role of Orbital Symmetry. *J. Am. Chem. Soc.* **1974**, *96*, 6755-6757.

(63) Glosík, J.; Skalský, V.; Praxmarer, C.; Smith, D.; Freysinger, W.; Lindinger, A. W. Dissociation of Kr^{+2}, N_2Ar^{+}, $(CO)^{+2}$, CH^{+5}, and C_2H^{+5} Ions Drifting in He. *J. Chem. Phys.* **1994**, *101*, 3792.

(64) Villano, S. M.; Eyet, N.; Wren, S. W.; Ellison, G. B.; Bierbaum, V. M.; Lineberger, W. C. Photoelectron Spectroscopy and Thermochemistry of the Peroxyformate Anion. *J. Phys. Chem. A* **2009**, *114*, 191-200.

(65) del Rio, E.; Lopez, R.; Sordo, T. L. A Theoretical Study of the H_2 Elimination from $C_2H_5^{+}$. *J. Phys. Chem. A* **1998**, *102*, 6831-6834.

(66) Stolte, W. C.; Ohrwall, G. Sulfur K-Edge Photofragmentation of Ethylene Sulfide. *J. Chem. Phys.* **2010**, *133*, 014306.

TOC